

Magnitude and oxidation potential of hydrocarbon gases released from the BP oil well blowout

Samantha B. Joye^{1*}, Ian R. MacDonald², Ira Leifer³ and Vernon Asper⁴

The deep-sea hydrocarbon discharge resulting from the BP oil well blowout in the northern Gulf of Mexico released large quantities of oil and gaseous hydrocarbons such as methane into the deep ocean. So far, estimates of hydrocarbon discharge have focused on the oil released, and have overlooked the quantity, fate and environmental impact of the gas¹. Gaseous hydrocarbons turn over slowly in the deep ocean, and microbial consumption of these gases could have a long-lasting impact on oceanic oxygen levels². Here, we combine published estimates of the volume of oil released^{1,3}, together with provisional estimates of the oil to gas ratio of the discharged fluid⁴, to determine the volume of gaseous hydrocarbons discharged during the spill. We estimate that the spill injected up to 500,000 t of gaseous hydrocarbons into the deep ocean and that these gaseous emissions comprised 40% of the total hydrocarbon discharge. Analysis of water around the wellhead revealed discrete layers of dissolved hydrocarbon gases between 1,000 and 1,300 m depth; concentrations exceeded background levels by up to 75,000 times. We suggest that microbial consumption of these gases could lead to the extensive and persistent depletion of oxygen in hydrocarbon-enriched waters.

The BP oil well blowout initiated a largely uncontrolled discharge from the Macondo prospect, a reservoir in Mississippi Canyon (MC252), northern Gulf of Mexico, containing at least 50–100 million barrels ($6.8\text{--}13.6 \times 10^6$ t) of oil⁵. This marine pollution event was unique because of the high hydrocarbon discharge rate, the extended duration (84 days), the depth of injection (1,480 m) and the fact that a substantial portion of the discharge was gaseous hydrocarbons. Previous oil discharges into the deep sea were from sunken ships with finite cargos, without concomitant release of gaseous hydrocarbons, or from well blowouts at depths within the oceanic mixed layer^{6,7} where gaseous hydrocarbons have efficient egress to the atmosphere⁸. Previous oil spills have been quantified in terms of the discharged liquid oil and have generally ignored gas.

The rate of hydrocarbon emission from the BP blowout has been debated widely⁹, but the ultimate release rate estimates from seabed video ranges from 62,500 (ref. 3) to 68,000 (ref. 1) barrels of oil per day (bopd) and the remote-sensing-derived upper limit estimate is 84,000 bopd (ref. 3). The uncertainty in these values is estimated to be 20% (ref. 3) for times when data were available; extrapolation to the duration of the spill increases this uncertainty as flow rates varied over time^{1,3}. Throughout this paper, the term barrel of oil refers to a 'standard barrel of oil', for example 42 US gallons or 159 l. The term 'Barrel of Oil Equivalent' (BOE) expresses the energy content of a barrel

of oil (6.1×10^6 kJ) and provides a mechanism to relate gaseous hydrocarbons and oil in equivalent units (for example, 1 BOE equals roughly 168 m^3 of natural gas).

For hydrocarbon discharges from well blowouts occurring at great depth, separation of gaseous and liquid hydrocarbon phases occurs during ascent towards the surface. Theoretical¹⁰ and experimental^{11,12} results indicate that some fraction of the hydrocarbons derived from such a deep discharge will be entrapped in layers hundreds of metres above the release depth; sub-surface hydrocarbon-rich layers result from even shallow blowouts (for example, the Ixtoc blowout)¹³. Here, we report an estimate for the total release of oil plus low-molecular-weight hydrocarbon gases, methane to pentane, during the BP discharge. We use BOE units to assess the total magnitude of hydrocarbons entering the ocean and present evidence for deep gas-rich layers resulting from the discharge. Finally, we consider the potential impact of these gaseous hydrocarbons on ocean biogeochemistry.

To determine gas magnitudes, we first used published estimates of oil release^{1,3} and a provisional estimate of the oil/gas ratio⁴ of 0.4. The gas was converted to BOE using the ideal gas equation, accounting for compressibility (a factor of 1.28; ref. 14; see Methods). We derived the total oil and gas fluxes (Table 1) and the flux of individual C_1 to C_5 gaseous hydrocarbons (Supplementary Tables S1 and S2). The gaseous hydrocarbon flux, $2.6\text{--}3.6 \times 10^5$ t or $1.6\text{--}1.9 \times 10^6$ BOE, increases the hydrocarbon flux calculated from oil alone ($5.9\text{--}8.4 \times 10^5$ t or $4.5\text{--}6.3 \times 10^6$ BOE; Table 1) substantially.

We then used reservoir yield data to derive an independent estimate of the gas flux. At the temperature (117°C) and pressure (825 bar) of the reservoir, hydrocarbon fluid is supercritical. The phase boundary between gas and oil develops as the fluid nears the seabed; it sharpens abruptly as the material exits the wellhead, and separates progressively as temperature and pressure change during ascent through the water column¹⁵. At a pressure of 1 bar and temperature of 15°C , $60\text{--}84 \text{ m}^3$ of gas was evolved per standard barrel of oil¹ (Patzek, T., personal communication). Using this gas volume and the oil release rate (corrected for gas recovery after 4 June 2010; see Methods) yields a gas discharge of $3.7\text{--}5.2 \times 10^5$ t or $2.2\text{--}3.1 \times 10^6$ BOE over the course of the spill (Table 1). The values generated using the reservoir data are higher, more than double in some cases, than those derived from the oil/gas ratio for a compressible gas. However, taken together, these calculations underscore the fact that a very large magnitude of low-molecular-weight hydrocarbon gases was injected into the deep ocean during the BP hydrocarbon discharge. Given the magnitude of the gas flux, understanding the fate of this material and its potential impact(s) on the oceanic system is essential.

¹Department of Marine Sciences, University of Georgia, Room 220 Marine Sciences Building, Athens, Georgia 30602-3636, USA, ²Department of Earth, Ocean and Atmospheric Science, Florida State University, Tallahassee, Florida 32306-4320, USA, ³Marine Science Institute, University of California, Santa Barbara, California 93106, USA, ⁴Department of Marine Science, University of Southern Mississippi, Stennis Space Center, Mississippi 39406, USA.

*e-mail: mjoye@uga.edu.

Table 1 | Oil and gas release from the BP blowout in equivalent units.

| Period of time | | A. Oil/gas ratio and ideal gas equation | | B. Gas/oil reservoir data | |
|--|----------------------|---|-----------|---------------------------|-----------|
| | | Mass (t) | BOE* | Mass (t) | BOE* |
| Phase I: 22 April–3 June 42 days | Oil low [†] | 349,732 | 2,625,000 | n.a. | n.a. |
| | Oil high | 470,040 | 3,528,000 | n.a. | n.a. |
| | Gas [‡] low | 151,565 | 912,935 | 217,901 | 1,312,500 |
| | Gas high | 203,703 | 1,226,984 | 292,859 | 1,764,000 |
| | Oil + gas low | 501,673 | 3,537,935 | n.a. | n.a. |
| | Oil + gas high | 673,744 | 4,754,984 | n.a. | n.a. |
| Phase II: 3 June–14 July [§] 42 days | Oil low | 247,722 | 1,859,337 | n.a. | n.a. |
| | Oil high | 368,030 | 2,762,337 | n.a. | n.a. |
| | Gas low | 107,356 | 646,649 | 154,343 | 929,669 |
| | Gas high | 159,495 | 680,815 | 229,301 | 1,381,169 |
| | Oil + gas low | 355,078 | 2,505,986 | n.a. | n.a. |
| | Oil + gas high | 527,525 | 3,443,152 | n.a. | n.a. |
| Total release 22 April–14 July 84 days | Oil low | 597,454 | 4,484,337 | n.a. | n.a. |
| | Oil high | 838,070 | 6,290,337 | n.a. | n.a. |
| | Gas low | 258,921 | 1,559,584 | 372,244 | 2,242,169 |
| | Gas high | 363,198 | 1,907,799 | 522,160 | 3,145,169 |
| | Oil + gas low | 856,751 | 6,043,921 | n.a. | n.a. |
| | Oil + gas high | 1,201,269 | 8,198,136 | n.a. | n.a. |

*BOE, Barrel of Oil Equivalent (U.S. Geological Survey standard conversion 6000 ft³ gas = 1 BOE at standard temperature and pressure).

[†]Calculated as the number of days times the daily oil release rate^{8,9}.

[‡]Total alkanes or the sum of methane, ethane, propane, butane and pentane concentration.

[§]Oil and gas release during phase II corrected for the amount captured/flared.

n.a. = not applicable.

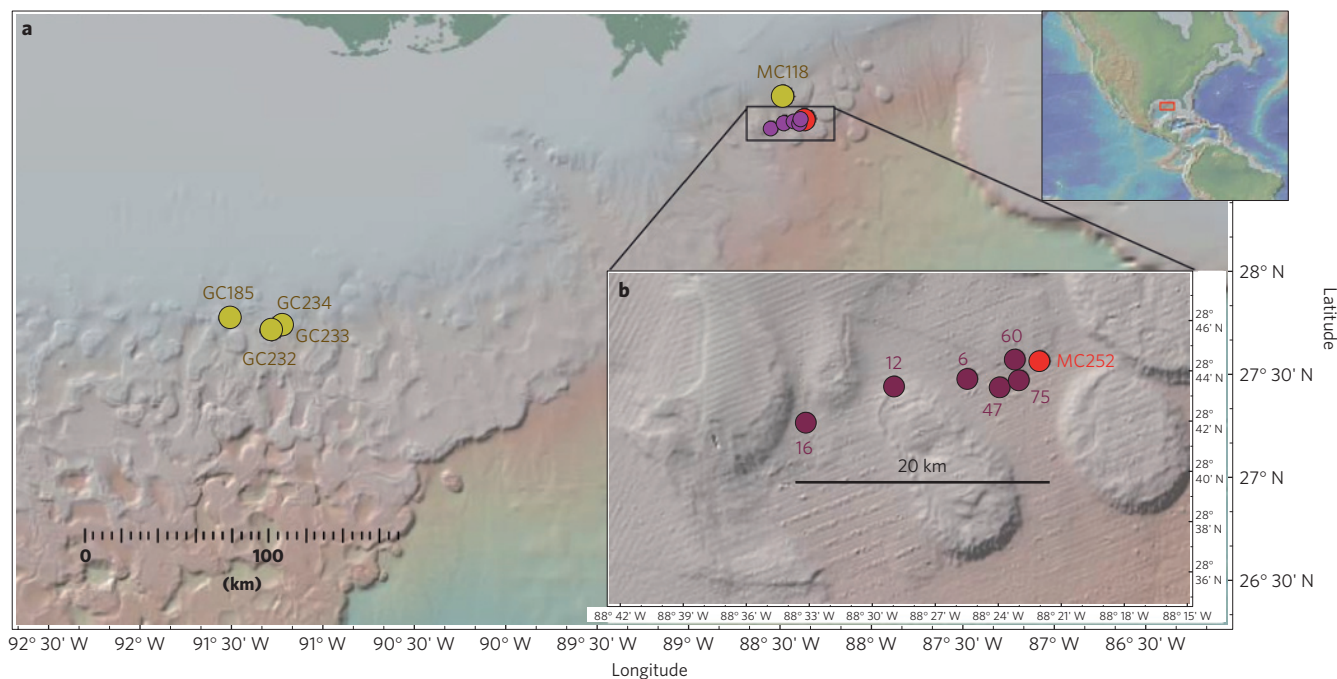


Figure 1 | Map of the study domain. a, b. Sites where reservoir alkane composition samples were collected (**a**) and where plume samples were collected in relation to the position of the wellhead (**b**).

Few researchers have attempted to model deep-sea emissions of oil and gas mixtures^{15,16}. Available numerical models of hydrocarbon behaviour following a deepwater blowout (that is, an oil and bubble plume) indicate that a large fraction of the gas is retained in deep waters⁸. At the temperature (4 °C) and pressure (153 bar) of the riser pipe, the solubility of methane gas in sea water is 135 mM (ref. 14). However, because the discharge was within

the gas hydrate stability zone, the solubility of methane in water is reduced (45 mM; ref. 17) and the discharged gas could either form gas hydrate or go into solution.

During a May/June 2010 research cruise on board the *R/V Walton Smith* (see Methods), we examined water-column hydrographic and optical signatures at 70 stations around the leaking wellhead; data from six representative stations are discussed

Table 2 | Alkane gas concentrations and potential oxidative oxygen demand.

| Station | Depth | Gas concentrations (nM) | | | | | $\Sigma C_1-C_5^*$ (nM) | O ₂ demand [†] (nM) | O ₂ demand (μ M) | O ₂ avail [‡] (μ M) | O ₂ avail [§] (% sat) | O ₂ demand (%) | |
|---------------------------|-------|-------------------------|--------|---------|------------------|------------|----------------------------|--|-------------------------------------|---|--|--|---------|
| | | Methane | Ethane | Propane | <i>n</i> -butane | Iso-butane | | | | | | | Pentane |
| Stations <5 km from MC252 | | | | | | | | | | | | | |
| WS60 | 1,000 | 193 | 14 | 7 | 24 | 20 | 62 | 320 | 1,250 | 1.2 | 170.94 | 54.10 | 0.7 |
| WS60 | 1,090 | 787 | 70 | 29 | 34 | 44 | 154 | 1,118 | 3,699 | 3.7 | 180.00 | 56.70 | 2.1 |
| WS60 | 1,160 | 186,702 | 18,158 | 11,365 | 1,891 | 3,788 | 449 | 222,353 | 534,288 | 534.3 | 171.97 | 53.88 | 310.7 |
| WS60 | 1,170 | 257,097 | 25,300 | 15,851 | 2,528 | 5,164 | 1,100 | 307,040 | 740,797 | 740.8 | 173.97 | 54.51 | 425.8 |
| WS60 | 1,310 | 21 | 0 | 6 | 30 | 14 | 38 | 110 | 667 | 0.7 | 196.25 | 61.30 | 0.3 |
| WS75 | 80 | 390 | 17 | 26 | 28 | 11 | 87 | 559 | 1,918 | 1.9 | 181.6 | 79.1 | 1.1 |
| WS75 | 1,050 | 39,706 | 4,020 | 2,810 | 520 | 990 | 463 | 48,509 | 121,051 | 121.1 | 175.9 | 55.6 | 68.8 |
| WS75 | 1,150 | 239,536 | 24,388 | 17,524 | 3,262 | 6,526 | 2,053 | 293,289 | 732,096 | 732.1 | 186.9 | 58.7 | 391.8 |
| WS75 | 1,205 | 139,218 | 14,576 | 10,538 | 1,829 | 3,301 | 992 | 170,454 | 423,423 | 423.4 | 190.8 | 59.7 | 221.9 |
| WS75 | 1,400 | 68 | 0 | 1 | 13 | 0 | 0 | 82 | 225 | 0.2 | 197.8 | 51.7 | 0.1 |
| WS47 | 80 | 14 | 0 | 0 | 0 | 0 | 0 | 14 | 28 | 0.0 | 181.6 | 79.1 | 0.0 |
| WS47 | 1,000 | 147 | 0 | 0 | 0 | 0 | 0 | 147 | 294 | 0.3 | 170.0 | 53.9 | 0.2 |
| WS47 | 1,110 | 46,826 | 4,486 | 3,168 | 560 | 1,434 | 654 | 57,128 | 143,386 | 143.4 | 181.6 | 57.1 | 79.0 |
| WS47 | 1,180 | 315,470 | 35,355 | 24,890 | 3,184 | 7,178 | 2,851 | 388,928 | 969,294 | 969.3 | 175.9 | 55.1 | 550.9 |
| WS47 | 1,400 | 57 | 0 | 15 | 14 | 0 | 0 | 86 | 278 | 0.3 | 199.7 | 62.3 | 0.1 |
| Stations >5 km from MC252 | | | | | | | | | | | | | |
| WS6 | 100 | 27 | 0 | 5 | 26 | 0 | 0 | 58 | 251 | 0.3 | 200.0 | 86.0 | 0.1 |
| WS6 | 600 | 11 | 0 | 6 | 0 | 16 | 42 | 75 | 492 | 0.5 | 123.13 | 41.26 | 0.4 |
| WS6 | 900 | 25 | 0 | 2 | 22 | 3 | 0 | 51 | 220 | 0.2 | 161.25 | 51.49 | 0.1 |
| WS6 | 1,020 | 743 | 58 | 6 | 28 | 9 | 19 | 862 | 2,108 | 2.1 | 170.94 | 54.21 | 1.2 |
| WS6 | 1,110 | 172 | 100 | 2 | 25 | 10 | 37 | 347 | 1,233 | 1.2 | 172.81 | 54.36 | 0.7 |
| WS6 | 1,300 | 27 | 2 | 8 | 0 | 0 | 8 | 45 | 164 | 0.2 | 189.38 | 61.51 | 0.1 |
| WS12 | 900 | 427 | 29 | 46 | 863 | 196 | 4 | 1,565 | 8,101 | 8.1 | 159.7 | 51.1 | 5.1 |
| WS12 | 1,020 | 45,956 | 4,480 | 3,146 | 1,879 | 1,802 | 1,316 | 58,579 | 157,777 | 157.8 | 174.7 | 55.3 | 90.3 |
| WS12 | 1,080 | 157,680 | 15,691 | 11,945 | 3,559 | 4,665 | 1,488 | 195,028 | 495,364 | 495.4 | 175.3 | 55.2 | 282.6 |
| WS12 | 1,140 | 210,171 | 20,338 | 13,156 | 2,966 | 3,946 | 1,238 | 251,815 | 612,137 | 612.1 | 165.3 | 51.9 | 370.3 |
| WS12 | 1,280 | 160,139 | 15,592 | 10,079 | 2,472 | 2,923 | 968 | 192,173 | 468,057 | 468.1 | 198.1 | 61.8 | 236.3 |
| WS16 | 100 | 15 | 0 | 3 | 13 | 0 | 0 | 31 | 128 | 0.1 | 203.4 | 86.4 | 0.1 |
| WS16 | 600 | 28 | 0 | 0 | 14 | 1 | 0 | 43 | 152 | 0.2 | 123.1 | 41.2 | 0.1 |
| WS16 | 1,025 | 594 | 0 | 3 | 14 | 1 | 0 | 612 | 1,301 | 1.3 | 166.6 | 52.7 | 0.8 |
| WS16 | 1,200 | 38 | 0 | 4 | 16 | 4 | 11 | 73 | 314 | 0.3 | 192.2 | 60.2 | 0.2 |
| WS16 | 1,300 | 373 | 45 | 41 | 49 | 0 | 9 | 516 | 1,494 | 1.5 | 166.9 | 5.3 | 0.9 |

*Sum of C₁ to C₅ alkane concentration (nM).

†Alkane-derived oxygen demand, calculated from equation (6), see text.

‡Measured oxygen concentration (μ M).

§Per cent oxygen relative to full saturation (100%).

|| Alkane oxygen demand divided by the oxygen available and then multiplied by 100.

here (Fig. 1, Supplementary Table S3). Compared with ambient deep-sea water in the Gulf of Mexico, we observed extraordinarily high concentrations of methane (up to \sim 300 μ M) and total alkanes (sum of methane to pentane; up to \sim 400 μ M; Table 2). The alkane-rich water occurred in horizontal plumes between 1,000 and 1,300 m below the sea surface and concentrations decreased with distance from the wellhead, indicating a localized-source discharge, namely the leaking riser pipe tapping the Macondo reservoir.

Methane concentrations observed within 20 km of the wellhead were 10^2 – 9×10^4 times those expected from equilibrium with the atmosphere (<4 nM) and 10 – 10^3 times those observed at naturally occurring Gulf of Mexico hydrocarbon seeps (4 nM–20 μ M; refs 18,19). Horizontal plumes were also characterized by strong fluorescence of coloured dissolved organic matter (CDOM), high beam attenuation, and in some cases dissolved oxygen depletion (Fig. 2). The strongest CDOM signals were proximal to the leaking wellhead whereas oxygen depletion and beam attenuation were highest away from the wellhead. The most strongly oxygen-depleted waters were characterized by lower concentrations of alkane gases

and weaker CDOM signals, providing potential signatures of oil and gas oxidation coupled to molecular oxygen consumption and oil dispersion (Fig. 2).

High-resolution digital photographs (see Methods) obtained throughout the water column at a site <3 km from the wellhead (near Station WS60) documented oil (Supplementary Fig. S1C) and gas hydrate (Supplementary Fig. S1D) within the water column. Above and below these oil/gas-rich layers, marine particles with a morphology that suggested they were floating upwards (Supplementary Fig. S1B, above the layer) or sinking downwards (below the layer, Supplementary Fig. S1D) were observed. The relative enrichment of C₂₊ to methane in the plume (Supplementary Table S4) is consistent with fractionation due to gas hydrate formation. The presence of gas hydrate in the water column helps explain both the presence of the deepwater plumes and the high gas concentrations observed within these plumes.

Low-molecular-weight alkane gases are oxidized by a variety of microorganisms, including *Methylosinus* sp. (CRL-15),

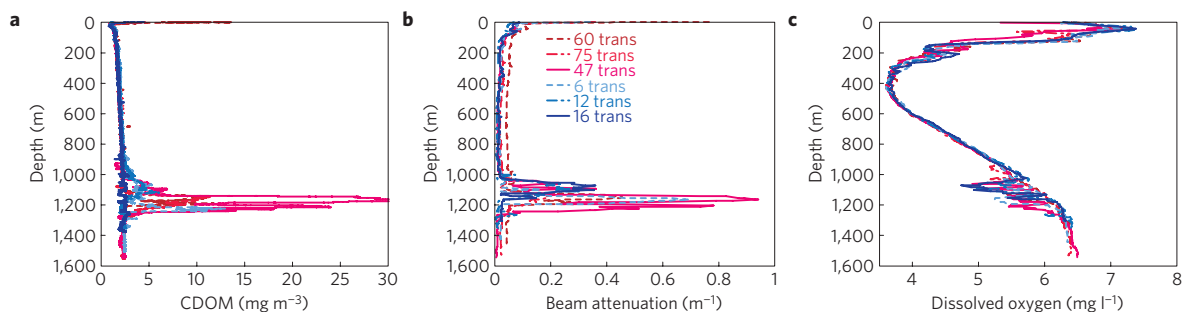
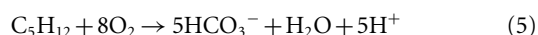
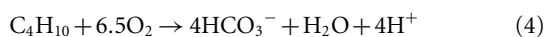
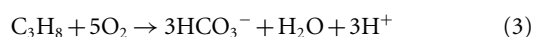
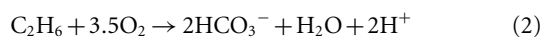
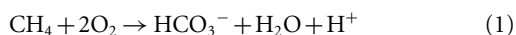


Figure 2 | Depth profiles through the water column. **a**, Depth distribution of CDOM signal (calibrated to quinone sulphate). **b**, Beam attenuation. **c**, Dissolved oxygen. Hot colours (red) denote stations within 5 km of the wellhead, whereas cold colours (blue) denote stations more than 5 km from the wellhead. The lines identifying stations are given in **b**.

Pseudomonas butanovora, *Gordonia* sp. (TY-5) and *Mycobacterium vaccae*^{20,21}. The oxidation of alkane gases coupled to the reduction of molecular oxygen generates bicarbonate, water and protons (equations (1)–(5)):



We estimated the amount of oxygen (nM) necessary to completely oxidize the alkanes measured within the plumes using equation (6):

$$\begin{aligned} \text{O}_2 \text{ demand} = & 2 \times [\text{CH}_4] + 3.5 \times [\text{C}_2\text{H}_6] + 5 \times [\text{C}_3\text{H}_8] \\ & + 6.5 \times [\text{C}_4\text{H}_{10}] + 8 \times [\text{C}_5\text{H}_{12}] \quad (6) \end{aligned}$$

Near the leaking wellhead (Station WS60), oxidation of the total dissolved alkane load in the plume core (307 μM ; 1,170 m) could generate an oxygen demand of 725 μM (Table 2). Sea water at this depth contained 174 μM oxygen; thus, the alkane-associated oxygen demand represents more than four times the available oxygen pool (Table 2). A total alkane concentration of 50 μM would deplete oxygen concentrations to below 63 μM , the level at which many oxygen-requiring animals become stressed, often with lethal consequences²². As alkane oxidation rates are low (typically picomoles per litre per day; refs 2,19), alkane consumption would require long time periods and as such, it is likely that gas input from the leaking wellhead could drive localized oxygen consumption and depletion in the deep ocean waters influenced by the discharge over long timescales (months to years). However, correlations between alkane and oxygen concentrations were poor because oil oxidation (dissolved and dispersed) also contributes to oxygen consumption in these plumes.

Four (Stations WS60, WS75, WS47 and WS12) of the five stations within 20 km of the leaking wellhead contained sufficient dissolved alkanes in horizontal plumes (1,100–1,300 m) to completely consume available oxygen (Table 2). At Station WS6, located 5.7 km from the wellhead, we observed a low potential alkane-oxidation-driven oxygen demand (Table 2) but depleted dissolved oxygen concentrations; the CDOM signal intensity was also lower. At Station WS16, some 20 km from the leaking wellhead, oxygen depletion was comparable to that observed at Station WS6, and plume water here contained the

lowest observed dissolved alkane concentrations and the weakest CDOM signals. The consistent pattern of low dissolved alkane concentrations and weak CDOM signals at stations with dissolved oxygen depletion indicates oxygen depletion driven by microbial consumption of these chemical species. These data underscore the critical need to better understand the physical dynamics of these features; to identify the pathways, rates and controls of microbial hydrocarbon metabolism; and to closely track plumes through time using a careful study design (to avoid under-sampling of these dynamic features).

Hydrocarbon inputs into the northern Gulf of Mexico from the BP discharge (5,000–10,000 t carbon per day from a single wellhead) contrast starkly with inputs from natural seepage (220–550 t carbon per day over the entire $7 \times 10^5 \text{ km}^2$ Gulf of Mexico system)⁷. Within the water column, natural seepage generates focused gas-rich plumes that extend for many hundreds of metres to kilometres into the water column^{15,23}. However, because natural seepage generates much lower dissolved alkane concentrations (usually nanomolar levels^{2,19}), water-column oxygen depletion has not been observed, except potentially near the bottom where alkane concentrations are highest^{8,24}. The BP discharge injected 24–400 times the basin-wide annual natural hydrocarbon flux from a localized source into oceanic waters around the Macondo prospect. The hydrocarbon fluxes in the wellhead region were at least seven orders of magnitude greater, on an aerial basis, than that generated by natural seepage processes.

The ultimate fate of plume hydrocarbons from the BP discharge and the impact on the oxygen budget of oceanic deep waters cannot be constrained at present. However, past periods of gas hydrate destabilization²⁵ and rapid methane release (for example, the Palaeocene/Eocene; Jurassic) stimulated activity of methane-consuming bacteria and led to formation hypoxic/anoxic bottom waters²⁶. Whether oxygen availability, nutrient availability or some other factor will limit microbial hydrocarbon consumption in the Gulf of Mexico remains unknown. However, available data indicate that alkane, light hydrocarbon, and oil consumption in the Gulf of Mexico deepwaters at a minimum could result in multiple, small-scale anoxic zones in areas affected by the BP blowout.

Quantifying the fate of hydrocarbons derived from the BP discharge and their ecological impact in the pelagic ocean and benthos process will provide valuable insight into the factors regulating the fate of methane and other hydrocarbons in the deep ocean, whether they derive from natural sources (hydrocarbon seeps) or human-induced (global-climate-change-induced hydrate destabilization or blowout) events.

Methods

The BP blowout was characterized by two distinct phases; the discharge began on 22 April 2010 and the well was capped on 15 July 2010. During Phase I (22 April–3 June), oil and gas flowed freely into Gulf of Mexico waters. During Phase II (4 June–15 July), some of the leaking oil and gas was recovered; phase II

fluxes presented here reflect oil and gas release minus recovery, that is, discharge (<http://www.energy.gov/open/oilspilldata.htm>).

The mass (tonnes carbon) and BOE of gas released from the well was calculated as follows. We used a low (62,500; ref. 3) and a high (84,000; ref. 3) estimate of bopd discharged, a provisional estimate of the volumetric oil to gas ratio at the sea floor (0.4; ref. 4), and converted barrels (42 gal) to cubic metres gas released per day. Next, cubic metres of gas at the sea floor was converted to moles of gas using the ideal gas equation ($n = PV/RT$, where $R = 8.314 \text{ m}^3 \text{ Pa mol}^{-1} \text{ K}^{-1}$, $P = 14.8 \times 10^6 \text{ Pa}$, $T = 277.15$ and $V =$ cubic metres of gas), corrected for the fact that methane is a non-ideal gas; thus, a correction for compressibility¹⁴ is necessary. Pressure and temperature data were obtained from conductivity, temperature and depth (CTD) data.

We estimated the relative proportion of individual C₁ to C₅ alkanes by multiplying the total moles of gas times the mass fraction for methane, ethane, propane, butane or pentane using data derived from several reservoirs in the Northern Gulf of Mexico (Supplementary Table S4). We converted moles of gas to the gas flux in tonnes carbon. To convert gas to BOE, we used the standard US Geological Survey conversion factor (1 BOE = 168 m³).

We also used the available data for the Macondo reservoir fluid^{9,27} (60–84 m³ of gas evolved per barrel of oil at standard temperature and pressure) and the estimates of oil release (bopd refs 1,3) to estimate cubic metres per day of gas evolved. Volumetric data were converted to tonnes as described above. In both calculations, total fluxes were calculated by multiplying daily flux by the number of days in the phase.

During the *R/V Walton Smith* cruise (25 May 2010 and 6 June 2010), a CTD–Niskin rosette system was used to obtain hydrographic profiles through the water column and bottle samples for alkane gas concentration determination. In addition to standard SeaBird temperature, pressure and conductivity sensors, the rosette was equipped with specific chemical sensors to document profiles of dissolved oxygen (SBE 43 Dissolved Oxygen Sensor), CDOM (WETLabs ECO FL CDOM fluorometer, EX 370 nm, EM 460 nm) and beam attenuation (WET Labs C-STAR transmissometer). All sensors were calibrated according to the manufacturer's specifications.

Niskin bottles were triggered at specific depths. On return to the surface, samples for dissolved alkane concentration analyses were collected immediately by attaching gas-tight tubing to the nozzle on the Niskin bottle. The tubing was fed into a 125 ml syringe, which had smaller diameter rubber tubing; the syringe was overfilled with three volumes to flush the syringe and tubing. The syringe was filled to the top, the plunger emplaced and the volume adjusted to 80 ml. Then, the tubing was placed into a helium-purged 125 ml glass serum vial containing two NaOH pellets. The water was transferred to a serum bottle (with minimal disturbance), which was then sealed quickly (blue rubber septum and crimp sealed); bottles were shaken vigorously to dissolve the base pellet, increasing pH and halting biological activity in the sample. Random field replicates were run and the variability between replicates was less than 4%.

Concentrations of C₁ to C₅ alkanes were determined using headspace extraction followed by gas chromatography. A 0.25 to 1 ml sub-sample was removed with a syringe and the sub-sample was injected into a gas chromatograph (model 8610C, SRI) equipped with a flame ionization detector. A temperature ramp was employed to elute C₃₊ alkanes. Sample concentrations were calculated by comparison to an alkane standard (Scott Specialty Gases) prepared in artificial sea water and treated exactly the same as samples. Variability between triplicate standards was <1%.

The marine snow photographic system consists of a pair of Deep Sea Power and Light collimated strobe lights that illuminate a 2-l water volume. Photographs of this volume are obtained using an Insite Pacific Scorpio 3.2 megapixel camera that acquired images every 10 s while being lowered at 10 m min⁻¹, resulting in a vertical spacing of 1.7 m. Images were deblurred using a Wiener filter in ImageJ (<http://rsbweb.nih.gov/ij/>). Depth was recorded using a Seabird Seacat CTD, equipped with a WETLabs C-Star transmissometer and a CDOM fluorometer.

Received 29 July 2010; accepted 17 December 2010;
published online 13 February 2011

References

- Crone, T. J. & Tolstoy, M. Magnitude of the 2010 Gulf of Mexico Oil Leak. *Science* **330**, 634 (2010).
- Valentine, D. L., Blanton, D. C., Reeburgh, W. S. & Kastner, M. Water column methane oxidation adjacent to an area of active hydrate dissociation, Eel River Basin. *Geochim. Cosmochim. Acta* **65**, 2633–2640 (2001).
- Leifer, I. *Deepwater Horizon Release Estimate of Rate by PIV* 67–106 (US Dept of Interior, 2010).
- Lehr, B. *et al.* *Deepwater Horizon Release Estimate of Rate by PIV* (Report to the US Dept of Interior, 2010).
- http://en.wikipedia.org/wiki/Macondo_Prospect (accessed 2 December 2010).
- Jernelöv, A. & Lindén, O. Ixtoc I: A case study of the world's largest oil spill. *Ambio* **10**, 299–306 (1981).
- National Research Council, Committee on Oil in the Sea. *Oil in the Sea III: Inputs, Fates and Effects*. (2003) ISBN: 0-309-50551-8.
- Leifer, I., Luyendyk, B. P., Boles, J. & Clark, J. F. Natural marine seepage blowout: Contribution to atmospheric methane. *Glob. Biogeochem. Cycles* **20**, GB3008 (2006).
- Achenbach, J. & Eilperin, J. Scientists offer varied estimates, all high, on size of BP oil leak. *The Washington Post* <http://go.nature.com/QtOrNp> (2010; accessed 2 December 2010).
- Zheng, L., Yapa, P. D. & Chen, F. H. A model for simulating deepwater oil and gas blowouts — Part I: Theory and model formulation. *J. Hydraulic Res.* **41**, 339–351 (2003).
- Chen, F. H. & Yapa, P. D. A model for simulating deepwater oil and gas blowouts—Part II: Comparison of numerical simulations with 'DeepSpill' field experiments. *J. Hydraulic Res.* **41**, 353–365 (2003).
- Masutani, S. M. & Adams, E. E. *Experimental Study of Multi-phase Plumes with Application to the Deep Ocean Oil Spills*. Contract No. 1435-01-98-CT-30964 (Final Report, US Department of the Interior Minerals Management Service, 2001).
- Boehm, P. D. & Fiest, D. Subsurface distributions of petroleum from an offshore well blowout: The IXTOC Blowout, Bay of Campeche. *Environ. Sci. Technol.* **16**, 67–74 (1982).
- Rehder, G., Leifer, I., Brewer, P. G., Friederich, G. & Peltzer, E. T. Controls on methane bubble dissolution inside and outside the hydrate stability field from open ocean field experiments and numerical modelling. *Mar. Chem.* **114**, 19–30 (2009).
- Leifer, I. & MacDonald, I. R. Dynamics of the gas flux from shallow gas hydrate deposits: Interaction between oily hydrate bubbles and the oceanic environment. *Earth Planet. Sci. Lett.* **210**, 411–424 (2003).
- Zheng, L. & Yapa, P. D. Modelling gas dissolution in deepwater oil/gas spills. *J. Mar. Syst.* **31**, 299–309 (2002).
- Duan, Z. & Mao, S. A thermodynamic model for calculating methane solubility, density, and gas phase composition of methane-bearing aqueous fluids from 273 to 523 K and 1 to 2000 bar. *Geochim. Cosmochim. Acta* **70**, 3369–3386 (2006).
- Solomon, E., Kastner, M., MacDonald, I. R. & Leifer, I. Considerable methane fluxes to the atmosphere from hydrocarbon seeps in the Gulf of Mexico. *Nature Geosci.* **2**, 561–565 (2009).
- Wankel, S. D. *et al.* New constraints on methane fluxes and rates of anaerobic methane oxidation in a Gulf of Mexico brine pool through the use of a deep sea *in situ* mass spectrometer. *Deep Sea Res.* **57**, 2022–2029 (2010).
- Head, I. M., Jones, D. M. & Roling, W. F. M. Marine microorganisms make a meal of oil. *Nature Rev. Microbiol.* **4**, 173–182 (2006).
- Rojo, F. Degradation of alkanes by bacteria. *Environ. Microbiol.* **11**, 2477–2490 (2009).
- Brewer, P. G. & Peltzer, E. T. Limits to marine life. *Science* **324**, 347–348 (2009).
- Greinert, J., Artemov, Y., Egorov, V., De Batist, M. & McGinnes, D. 1300-m-high rising bubbles from mud volcanoes at 2080 m in the Black Sea: Hydroacoustic characteristics and temporal variability. *Earth Planet. Sci. Lett.* **244**, 1–15 (2006).
- Jochens, A. E. *et al.* *Understanding the Processes that Maintain the Oxygen Levels in the Deep Gulf of Mexico: Synthesis Report*. OCS Study MMS 2005-032 (US Dept. of the Interior, Minerals Management Service, Gulf of Mexico OCS Region, 2005).
- Dickens, G. R., Castillo, M. M. & Walker, J. C. G. A blast of gas in the latest Paleocene: Simulating first order effects of massive dissociation of oceanic methane hydrates. *Geology* **25**, 259–262 (1997).
- Hesselbo, S. P. *et al.* Massive dissociation of gas hydrate during a Jurassic oceanic anoxic event. *Nature* **406**, 392–395 (2000).
- Ahmed, T. H. *Hydrocarbon Phase Behaviour* (Gulf Publishing Company, 1989).

Acknowledgements

This research was supported by the US National Science Foundation's Biological and Chemical Oceanography Programs (OCE-1043225 to S.B.J.) and the NOAA National Institute for Undersea Science and Technology (award numbers 0710028 and 0810031 to S.B.J. and I.R.M.). We thank J. Slaughter (UGA) for analytical assistance and K. Bowles, M. Bowles and C. Meile for providing comments that substantially improved the manuscript.

Author contributions

S.B.J. and V.A. participated in the cruise; S.B.J., I.R.M. and I.L. carried out the gas flux calculations; S.B.J. wrote the paper and other authors provided comments/feedback.

Additional information

The authors declare no competing financial interests. Supplementary information accompanies this paper on www.nature.com/naturegeoscience. Reprints and permissions information is available online at <http://npg.nature.com/reprintsandpermissions>. Correspondence and requests for materials should be addressed to S.B.J.